Celal Bayar University Journal of Science

Evaluation of the thermal performance of a cold plate with different fin structures for IGBT cooling

Mehmet Bahattin Akgül[1]*, Furkan Sinan Erçel[2]

[1] Department of Mechanical Engineering, Manisa Celal Bayar University, 45140 Muradiye, Manisa, Türkiye
[2] R&D Department, Coşkunöz Kalıp Makine, 16000 Nilüfer, Bursa, Türkiye
* mbakgul@gmail.com
* Orcid No: 0000-0002-8916-1171

Received: July 2, 2025
Accepted: August 1, 2025
DOI: 10.18466/cbayarfbe.1732854

Abstract

Insulated Gate Bipolar Transistor (IGBT) modules are a frequently used switching and power control element in power electronics. A significant amount of heat is released due to conduction and switching losses inside the module. To ensure the efficient and long-term operation of the IGBT, the heat generated must be cooled effectively. Forced liquid cooled cold plates are widely used for high power density modules. In this study, a cold plate is designed for liquid cooling of three PrimePack3 IGBTs used in an industrial motor drive. Straight, staggered pin and oblique fin structures are applied to the cooling channels of the cold plate with a parallel flow configuration. The numerical model of the cold plate is developed and analyzed using a CFD software. The effects of fin structures on liquid cooling performance are compared and discussed in detail. The thermal resistance values for the staggered pin and oblique fin structures exhibit reductions of 46.5% and 60.1%, respectively, compared to the straight fin configuration.

Keywords: Cold Plate, IGBT, Liquid Cooling, CFD, Pin Fin, Straight Fin, Oblique Fin

1. Introduction

Insulated Gate Bipolar Transistor (IGBT) modules are one of the most fundamental components in power electronics applications. IGBTs are used for power and speed control in many areas such as electric vehicles, renewable energy, motor drives and industrial machinery. The modules generate a significant amount of heat due to conduction and switching losses while regulating current and voltage levels. Due to the semiconductor structure of the modules, the junction temperatures must be at a certain level in order for reliable operation [1-3]. Air or two phase (heat pipes or vapor chambers) cooling systems are employed for low power level IGBT modules [4-12]. In high power applications, liquid cooling is applied due to its high heat transfer capacity and homogeneous temperature distribution [13,14]. The liquid cooling system consists of a cold plate (CP) that transfers heat directly from the modules to the coolant, a pump that facilitates coolant circulation, a radiator that transfers the heat to the ambient air, and auxiliary equipments.

The fin structures, coolant channel configurations, and flow characteristics in CP have significant effects on cooling performance [15-22]. Yang et al. [23] investigated the performance of a CP with z-type parallel channels supported by phase change materials for battery cooling systems. They reported that the phase change material supported hybrid cold plate achieves the same heat transfer at 40% lower pumping power. Om et al. [24] investigated the heat transfer of inclined fins in a CP for in-line, inclined and louvered arrangements. They showed that they obtained a homogeneous temperature distribution with the inclined fin structure. They found the highest Nusselt number with the louvered inclined fin arrangement. Wiriyasart and Naphon [25] investigated the effect of prismatic, cylindrical and conical fin structures on heat transfer in CP for water and nanofluids. They obtained the lowest surface temperature for both coolants in the conical fin structure. Zhang et al. [26] designed a mini-channel CP for the liquid cooling of high-heat-flux electronic devices. They conducted a heat transfer analysis for cooling channels with zigzag, square-wave, and wavy configurations within the mini-channel. They observed a 12°C reduction in surface temperatures with the zigzag counter-flow channel configuration compared to straight channels. Imran et al. [27] aimed to enhance cooling performance by designing the liquid channels within a CP to follow the form of the flow streamline. They achieved up to a 12%

improvement in the Nusselt number with the new channel configuration. Ren et al. [28] designed a new CP using topology optimization. They reported that the maximum surface temperature of the new CP was reduced by 12% compared to the flat mini-channel plate. Jiang et al. [29] placed square, triangular, semicircular, and trapezoidal ribs into the flow channels of a CP to reduce pressure drop. They found that the rib structures resulted in a 2.1-fold increase in heat transfer compared to a straight-channel configuration. Pandey et al. [30] investigated the effects of pin-shaped fins on heat transfer and pressure drop in a CP with parallel flow channels. They reported a decrease of up to 92% in maximum temperatures against a 60% increase in pressure drop in the pin fin configuration.

The above literature review includes extensive studies for liquid cooling of electronic devices using CPs. Considering manufacturing and cost constraints, there is a lack of studies investigating the effects of different fin structures in cold plates with parallel flow configurations. In this study, a parallel flow CP is designed for liquid cooling of three PrimePack3 IGBTs used in an industrial motor drive straight, staggered pin and oblique fin structures are applied to the coolant flow channels. A simulation model of the CP based on the finite volume method has been developed. For each configuration, maximum and average temperatures, as well as pressure drops, were determined at different coolant flow rates. Improvements in heat transfer have been presented graphically and discussed in detail.

2. Geometry of the CP models

The rectangular CP, with dimensions of 350 mm x 390 mm x 14 mm as shown in Fig. 1, is manufactured from aluminum 6063 alloy using the CNC milling method. The three PrimePack3 IGBT modules are mounted on the CP top surface. The CP consist of a main block containing cooling channels, a cover, and adapters that facilitate coolant inlet and outlet. The coolant is a mixture of 50% ethylene glycol and 50% pure water by volume. The thermophysical properties of the CP material and coolant are given in Table 1.

Table 1. Material Properties

Material	Density ($kg \cdot m^{-3}$)	Specific Heat (J/(kgK))	Dynamic Viscosity (Pa.s)	Thermal Conductivity (W/mK)
Al 6063	2700	900	-	200
Coolant	1045	3425	0.002	0.41

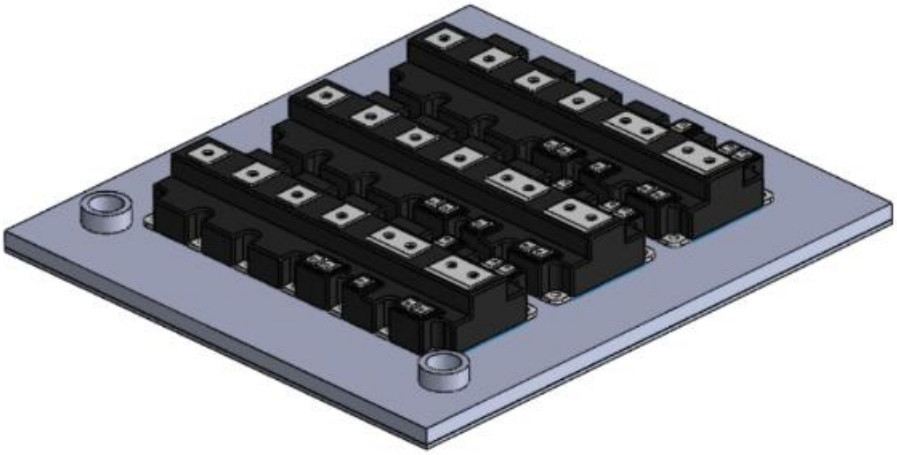

Figure 1. IGBT mounted CP

The structure of straight, staggered pin and oblique fin structures in the CP with parallel flow configuration is given in Fig. 2. All fin arrangements are set with a flow channel width of 3.5 mm and a height of 8 mm. The angle of inclination of the oblique fin is considered as 60°.

Celal Bayar University Journal of Science
Volume 21, Issue 3, 2025, p 80-88
Doi: 10.18466/cbayarfbe.1732854

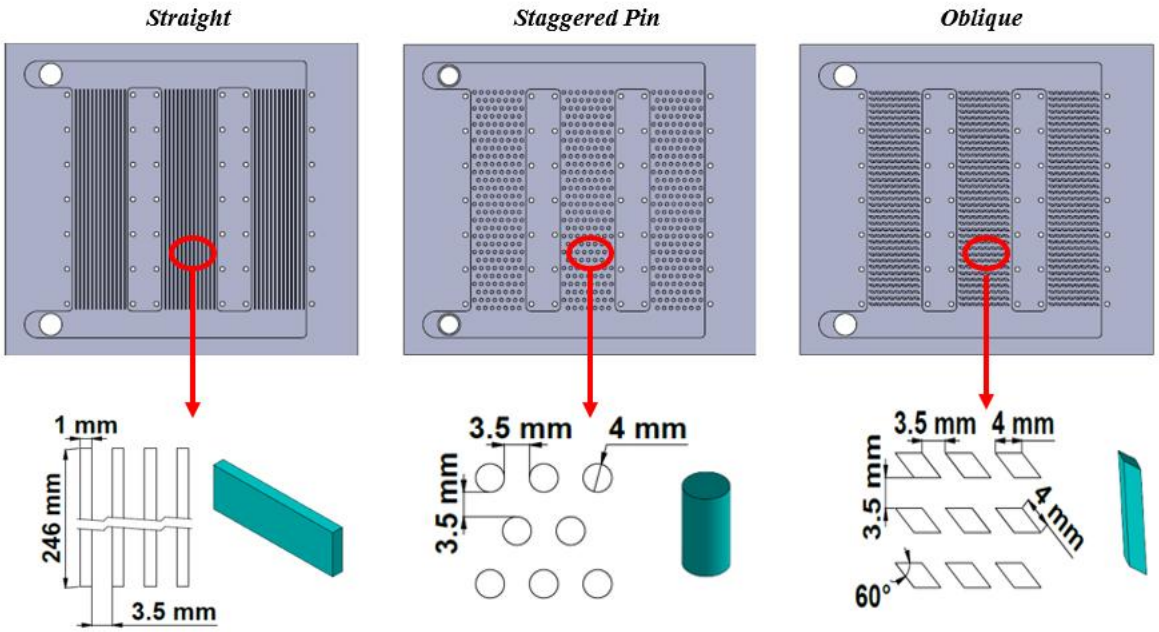

Figure 2. Fin structures in parallel flow CP

3. Numerical Analysis and Data Reduction

A three-dimensional numerical model has been developed to better understanding of the flow field and heat transfer characteristics of CP configurations in liquid cooling systems of IGBTs. The following assumptions are taken into account in the construction of the simulation model: (1) the flow is three-dimensional, incompressible and steady state; (2) the thermo-physical properties of the liquid are assumed constant; (3) radiation and natural convection effects are neglected; (4) heat transfer occurs only between the cold plate and the liquid.

Using the above assumptions, the main equations for the simulation model can be expressed as follows:

Continuity equation:

$$\nabla.\vec{V} = 0 \tag{1}$$

Momentum equation:

$$\rho_f \left(\vec{V}.\nabla\vec{V}\right) = \left(\mu_f + \mu_t\right)\cdot\nabla^2\,\vec{V} - \nabla p \tag{2}$$

Energy equations for the liquid and solid domains (coolant and CP) are respectively given as:

$$\rho_f c_{p,f}(\vec{V}.\nabla T) = k_f \nabla^2 T \tag{3}$$

$$k_s \nabla^2 T = 0 \tag{4}$$

where, ρ_f is the coolant density, k_f and k_s are the thermal conductivities of the coolant and CP solid material, respectively. $c_{p,f}$ is the specific heat of the coolant. *P, V* and *T* are the pressure, velocity vector, and temperature, respectively. In the momentum equation, μ_f and μ_t are the viscosities of the coolant and eddy, respectively. The standard k-epsilon model is used for turbulence modeling as follows:

$$\rho_f \frac{\partial}{\partial x_i}(k_t V_i) = \frac{\partial}{\partial x_j}\left[\left(\mu_f + \frac{\mu_t}{\sigma_k}\right)\frac{\partial k_t}{\partial x_j}\right] + P_k - \rho_f \varepsilon \tag{5}$$

$$\rho_f \frac{\partial}{\partial x_i}(\varepsilon V_i) = \frac{\partial}{\partial x_j}\left[\left(\mu_f + \frac{\mu_t}{\sigma_\varepsilon}\right)\frac{\partial \varepsilon}{\partial x_j}\right] + C_{1\varepsilon}\frac{\varepsilon}{k_t}P_k - C_{2\varepsilon}\rho_f\frac{\varepsilon^2}{k_t} \tag{6}$$

where, $\mu_t = \rho_f C_\mu \frac{{k_t}^2}{\varepsilon}$, $P_k = \mu_t \frac{\partial V_i}{\partial x_j}\left(\frac{\partial V_i}{\partial x_j} + \frac{\partial V_j}{\partial x_i}\right)$

The empirical constants are [31]:

$C_\mu = 0.09$, $C_{1\varepsilon} = 1.44$, $C_{2\varepsilon} = 1.92$ and $\sigma_\epsilon = 1.3$

The CFD tool used for the numerical analysis is Simcenter FLOEFD. The SIMPLE algorithm is used to obtain the velocity and pressure couplings between the momentum and mass conservation equations. The pressure, momentum and energy equations are discretized by a second order upwind scheme. The iterative solution is performed with convergence targets of 10^{-6} for the energy equation and 10^{-3} for the continuity and momentum equations. The boundary conditions of the solution domain are presented in Fig. 3 and compiled in detail in Table 2.

Celal Bayar University Journal of Science
Volume 21, Issue 3, 2025, p 80-88
Doi: 10.18466/cbayarfbe.1732854

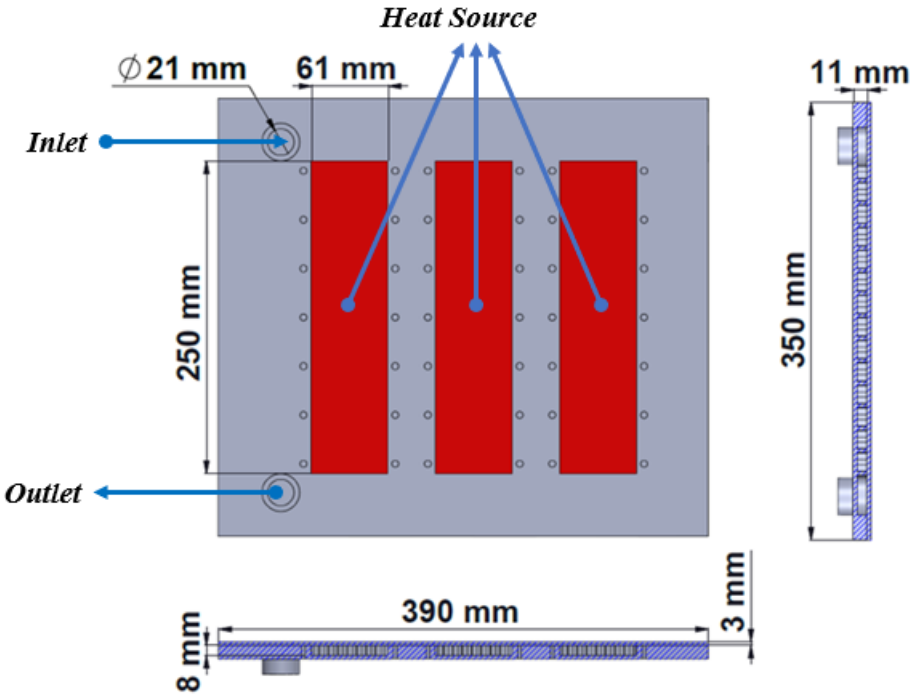

Figure 3. Boundary conditions for computational domain

Table 2. Details of the boundary conditions

Boundary	Parameter	Value
Inlet	Volume flow rate	Ranges from 20-30 l/min
Inlet	Temperature	25 ^{0}C
Outlet	Pressure outlet	0 Pa
Fluid-solid interface surface	Coupled wall	-
IGBTs mounting surfaces	Constant heat source	1800 W for per IGBT
Other surfaces	Adiabatic	-

The thermal performance of the CP is generally related to the main parameters such as pressure drop, maximum surface temperature, thermal resistance, and performance evaluation criteria (PEC). The thermal resistance of the CP is computed using the equation:

$$R_{th} = \frac{T_{max} - T_{in}}{Q} \quad (7)$$

In order to compare the hydrothermal performance of the CP with staggered pin and oblique fin structures with that of the CP with straight fins, the Performance Evaluation Criterion (PEC) was calculated as follows:

$$PEC = \frac{R_0/R}{(\Delta P/\Delta P_0)^{1/3}} \quad (8)$$

where T_{max} is the maximum surface temperature of the CP, Q is the heat load of the IGBTs, T_{in} is the coolant inlet temperature, ΔP and $\dot{V}$ are the pressure drop and flow rate of the coolant, respectively.

A grid structure has been established within the computational domain using hexahedral elements. To enhance the accuracy of the simulation, a high-resolution mesh has been employed particularly in the boundary layer region. The details of this grid configuration are presented in Fig. 4. For the grid independence study, a range of total grid sizes, namely 0.6, 0.8, 1.3, 1.97, 2.25 and 2.6 million elements, has been used across the computational domain. The objective of this grid dependence analysis is to achieve a precise solution while minimizing the number of elements. The outcomes of the grid independence study are illustrated in Fig. 5. The results indicate that, beyond a grid size of 1.97 million elements, further refinement of the grid has a negligible impact on both pressure drop and temperature.

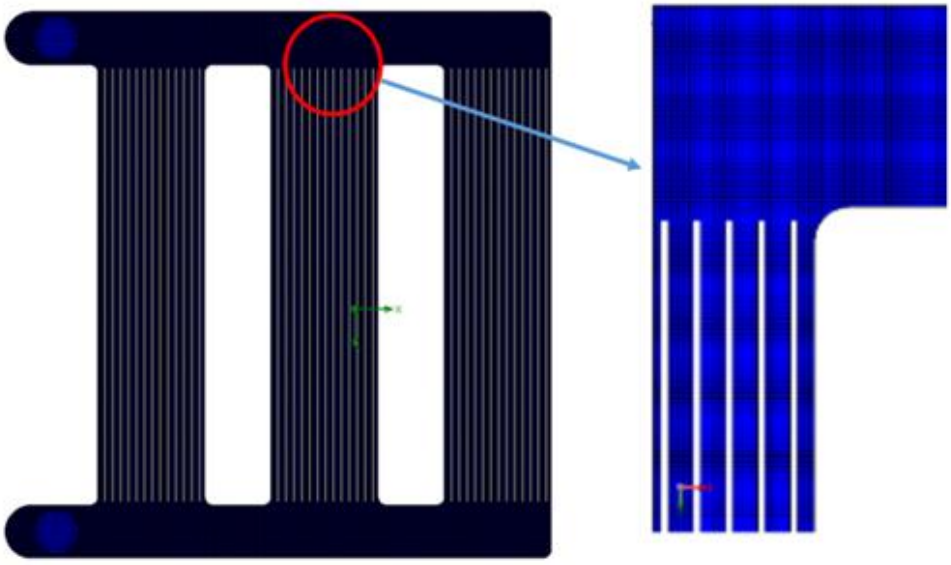

Figure 4. Grid structure

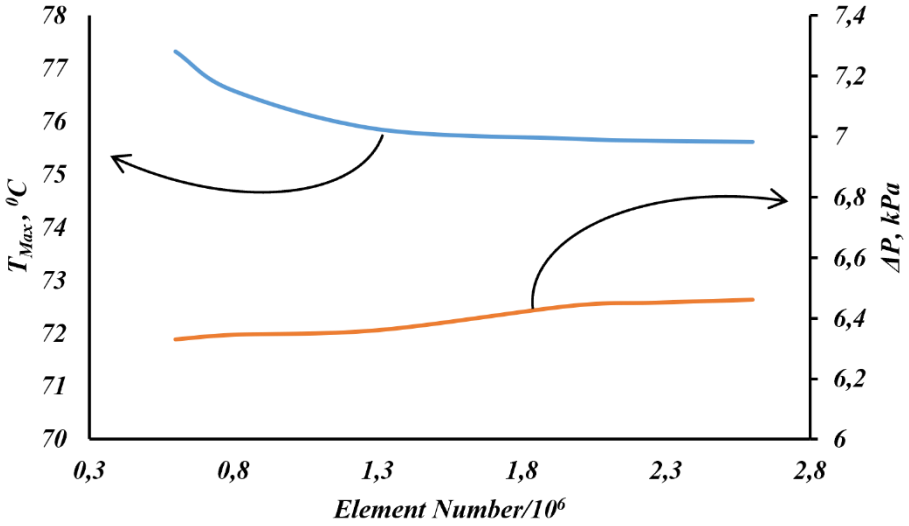

Figure 5. Effects of element number on the pressure drop and surface temperature.

4. Results

Thermal performance analysis of a CP with three different fin structures has been carried out for different flow rates. Design parameters such as thermal resistance and pumping power are compared and analyzed for all three cases. Surface temperature and velocity distribution of the cold plate are given in Fig. 6 for coolant flow rate of 25 l/min. The maximum temperature value for the CP with straight fin configuration is 72.66 °C, while it is 51.23 °C and 44.9 °C for the staggered pin and oblique fin structures, respectively. In the straight fin configuration, hot-spot zones are formed as can be clearly seen in the figure.

Celal Bayar University Journal of Science
Volume 21, Issue 3, 2025, p 80-88
Doi: 10.18466/cbayarfbe.1732854

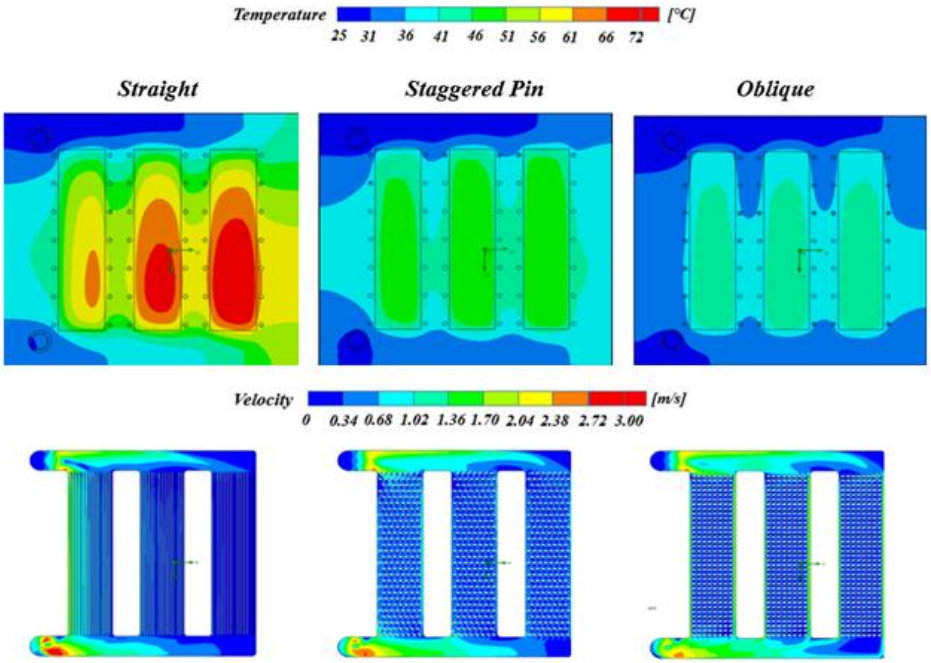

Figure 6. Temperature and velocity distributions for different fin structures.

In relation to the velocity contour plot, the staggered pin and oblique fin cases show a much more homogeneous temperature distribution due to increased turbulence effects. Fig. 7 shows the variation of the maximum CP surface temperature with flow rate for three different fin configurations. The straight fin configuration gives the highest surface temperature values ranging from 75.67 °C at 20 LPM to 70.65 °C at 32 LPM. In the staggered pin configuration, the temperature decreases from 53.78 °C to 49.3 °C for the same flow rates. In the oblique fin configuration, the maximum surface temperatures drop to 43.20°C at 30 LPM due to the homogeneous distribution of the coolant.

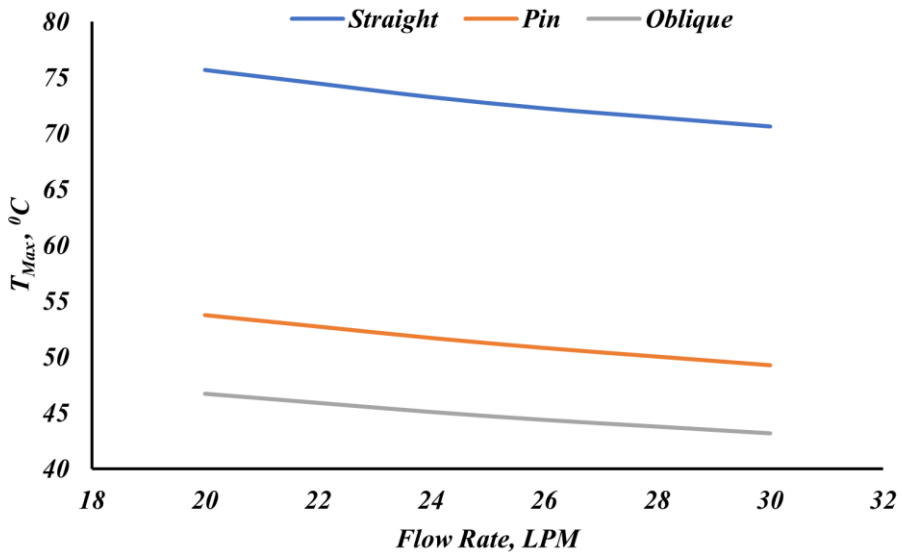

Figure 7. Maximum surface temperature with flow rate.

The effect of the coolant flow rate on the thermal resistance is shown in Fig. 8 for different fin structures. As can be clearly seen from the figure, the thermal resistance decreases with increasing flow rate due to the improvement of the heat transfer coefficient. Significant reduction in thermal resistance values is obtained for staggered pin and oblique fin structures compared to straight fin. For 30 LPM, the thermal resistance values for staggered pin and oblique fin structures are 0.013 and 0.010 °C/W, respectively.

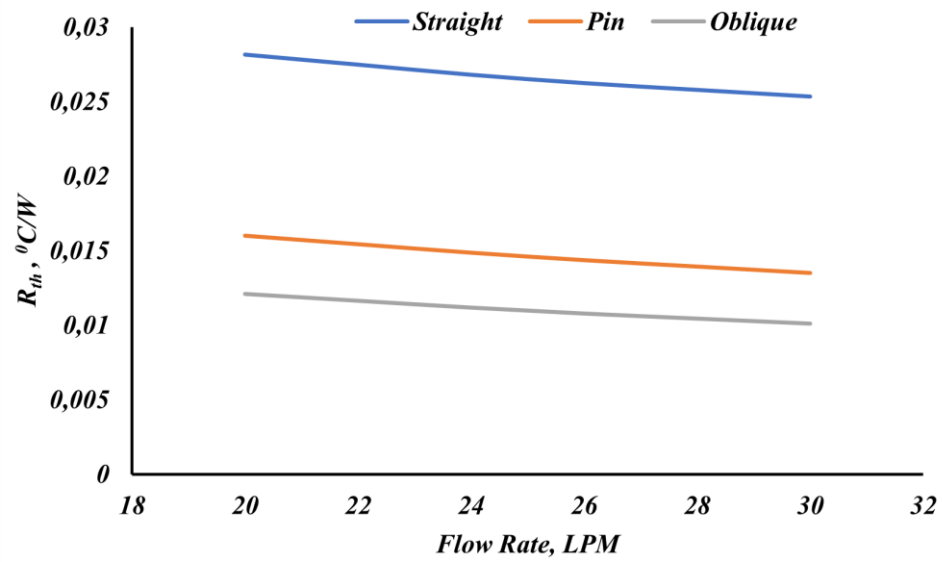

Figure 8. Thermal resistance values versus flow rate.

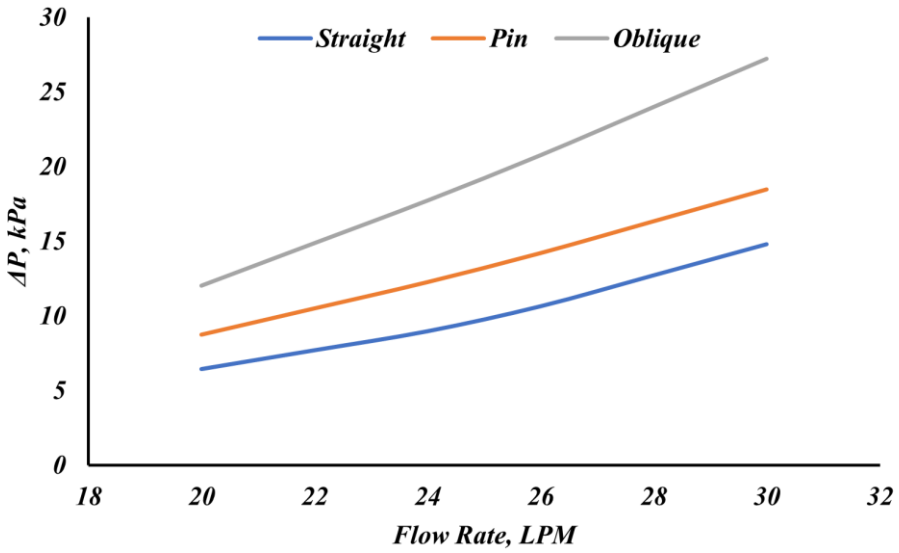

Figure 9. Pressure drop values versus flow rate.

Fig. 9 shows the variation in pressure drop with flow rate for three different fin structures. As expected, the pressure drop increases with increasing of the flow rate. According to the CFD simulation results, the highest-pressure drop of approximately 27.24 kPa was obtained for 30 LPM in the oblique fin structure. The rate of increase in the pressure drop shows a similar trend in the straight and pin structures, while it is larger in the oblique fin structure. Finally, the improvement in the hydrothermal performance of the CPs with different fin structures is characterized by a general index, the performance evaluation criterion (PEC). This dimensionless index is used to compare the performance of the staggered pin and oblique fin configurations with the straight fin structure as shown in Fig. 10. It is clear that staggered pin and oblique fin structures provide significant improvements in thermal performance compared to straight fins. Despite the high pressure drops in the oblique fin structure, heat transfer is significantly increased due to the homogeneous distribution of the coolant between the fins, allowing higher PEC values to be obtained.

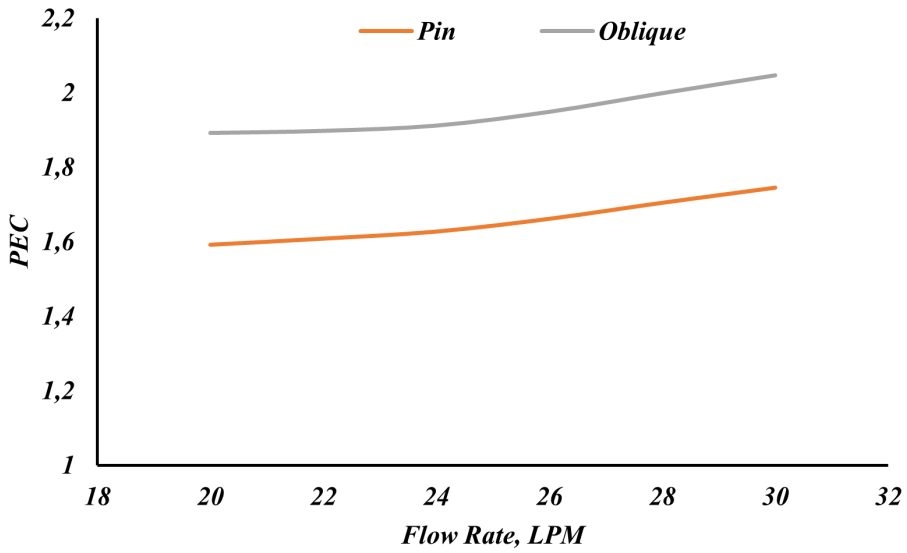

Figure 10. PEC values versus flow rate.

5. Conclusion

The hydrothermal performance of a parallel-flow cold plate (CP) designed for liquid cooling of three PrimePack3 IGBT modules in an industrial motor drive is comprehensively evaluated, including straight, staggered pin and inclined fin structures. As a result of the study, the main conclusions are summarized below:

- The lowest surface temperature of 43.20 °C for 30 LPM is obtained for the oblique fin structure.
- The thermal resistance values for the staggered pin and oblique fin structures exhibit reductions of 46.5% and 60.1%, respectively, compared to the straight fin configuration.
- The highest-pressure drop of 27.24 kPa at 30 LPM is observed in the oblique fin structure.
- The optimal thermal performance is observed in the oblique fin configuration. The pin fin structure exhibits an intermediate thermal performance, while the worst performance is found to occur in the straight fin configuration.

It can be concluded that the superior thermal performance demonstrated by the oblique fin configuration highlights its potential as an optimal design choice for enhancing the efficiency of CP systems in high-power IGBT applications.

Author's Contributions

Mehmet Bahattin Akgül: Drafted and wrote the manuscript, performed the result analysis, performed the analytic calculations and performed the numerical simulations.

Furkan Sinan Erçel: Assisted in analytical analysis on the structure and helped in manuscript preparation.

Ethics

There are no ethical issues after the publication of this manuscript.

References

[1]. X, Perpina, J. Serviere, X. Jorda, A. Fauquet, S. Hidalgo, J. Urresti-Ibanez, et al., IGBT module failure analysis in railway applications. Microelectron. Reliab. 48 (2008) 1427–31.

[2]. M. Ciappa, A. Castellazzi, Reliability of high-power IGBT modules for traction applications, Int. Rel. Phys. Symp. Proc (2007) 480–485.

[3]. C. Qian, A.M. Gheitaghy, J. Fan, H. Tang, B. Sun, H. Ye, G. Zhang, Thermal management on IGBT power electronic devices and modules, IEEE Access 6 (2018) 12868–12884.

[4.] H. Tang, Y. Tang, Z. Wan, J. Li, W. Yuan, L. Lu, Y. Li, K. Tang, Review of applications and developments of ultra-thin micro heat pipes for electronic cooling, Appl. Energy 223 (2018) 383–400.

[5]. G. Li, J. Zhang, J. Gao, Thermal Analysis and Structural Optimization of Dual IGBT Module Heat Sink under Forced Air Cooling Condition, in: 2019 IEEE 3rd Advanced Information Management, Communicates, Electronic and Automation Control Conference (IMCEC), 2019.

[6]. B. Wang, S. Member, L. Wang, S. Member, F. Yang, W. Mu, M. Qin, S. Member, F. Zhang, D. Ma, J. Wang, J. Liu, Air-cooling system optimization for IGBT modules in MMC using embedded O-shaped heat pipes, IEEE J. Emerg. Sel. Top. Power Electron. 9 (2021) 3992–4003.

[7]. Y. Zhao, Z. Liu, Z. Quan, et al., Thermal management and multi-objective optimization of an air-cooled heat sink based on flat miniature-heat-pipe arrays, J. Therm. Anal. Calorim. 149 (5) (2024) 2443–2462.

[8]. X. Zhao, J. Sun, C. Wang, Z. Zhang, Experimental and numerical study of electronic module-cooling heat sinks used in a variable frequency air-conditioner outdoor unit, Int. J. Refrig 38 (2014) 10–21.

[9]. S.H. Kim, C.S. Heu, J.Y. Mok, S.-W. Kang, D.R. Kim, Enhanced thermal performance of phase change material-integrated fin-type heat sinks for high power electronics cooling, Int. J. Heat Mass Transf. 184 (2022) 122257.

[10]. Y.E. Nikolaenko, A.V. Baranyuk, S.A. Reva, E.N. Pis ′ mennyi, F.F. Dubrovka, V. A. Rohachov, Improving air cooling efficiency of transmit/receive modules through using heat pipes, Therm. Sci. Eng. Prog. 14 (2019) 100418.

[11]. Y. Chen, B. Li, X. Wang, et al., Investigation of heat transfer and thermal stresses of novel thermal management system integrated with vapour chamber for IGBT power module, Thermal Science and Engineering Progress. 10 (2019) 73–81.

[12]. Y. Ren, W. Luo, Z. He, N. Qin, Q. Meng, M. Qiu, et al., Development and performance study of a radiation-enhanced heat pipe radiator for cooling high- power IGBT modules, Appl. Therm. Eng. 262 (2025), 125307, https://doi.org/ 10.1016/j.applthermaleng.2024.125307

[13]. S. Ki, J. Lee, S. Ryu, S. Bang, K. Kim, Y. Nam, A bio-inspired, low pressure drop liquid cooling system for high-power IGBT modules for EV/HEV applications, Int. J. Therm. Sci. 161 (2021) 106708.

[14]. M. Katagiri, K. Mae, Y. Nishimura, Y. Yasuda, T. Yamauchi, Development of liquid cooling system with integrated traction converters and auxiliary power supplies for 200-km/h commuter trains, 2017, https://www.hitachi.com/rev/archive/2017/r2017_02/10/index.html.

[15]. M. Parlak, A. ¨Ozsunar, A. Kosar, High aspect ratio microchannel heat sink optimization under thermally developing flow conditions based on minimum power consumption, Appl. Therm. Eng. 201 (2022), 117700.

[16]. M.B. Akgül, F.S. Erçel, Thermal Performance Analysis of a Liquid Cooling Plate for Power Electronics. Celal Bayar Üniversitesi Fen Bilimleri Dergisi 20.4 (2024): 72-81.

[17]. W. Jiang, J. Zhao, Z. Rao, Heat transfer performance enhancement of liquid cold plate based on mini V-shaped rib for battery thermal management, Appl. Therm. Eng. 189 (2021), 116729.

[18]. X. Mo, H. Zhi, Y. Xiao, H. Hua, L. He, Topology optimization of cooling plates for battery thermal management, Int. J. Heat Mass Tran. 178 (2021) 121612.

[19]. X. Cao, H.-L. Liu, X.-D. Shao, H. Shen, G. Xie, Thermal performance of double serpentine minichannel heat sinks: Effects of inlet-outlet arrangements and through-holes, Int. J. Heat Mass Transf. 153 (2020) 119575.

[20] B. Zhan, H. Xu, H. Zhang, D. Leng, C. Tian, Y. Zhou, Research and optimization of liquid cooling plate for high-heat-flux components, J. Refriger. 42 (2) (2021) 69–76.

[21] H. Dai, T. Wenbin, H. Min, S. Liu, C. Zhang, Z. Wei, Z. Dong, C. S. Chin, Enhancing thermal management in electric commercial vehicles: A novel liquid-cooled Multiple Parallel-Serpentine channels. Journal of Energy Storage 107 (2025): 114708.

[22]. M. Pang, J. Liu, W. Liu, et al., Thermal-and-energy-conservation optimization of the cooling plate for IGBT by field synergy and entropy generation, Int. J. Heat Fluid Flow 108 (2024) 109453.

[23]. H. Yang, M. Li, Z. Wang, B. Ma, A compact and lightweight hybrid liquid cooling system coupling with Z-type cold plates and PCM composite for battery thermal management, Energy 263 (2023), 126026.

[24]. N.I. Om, R. Zulkifli, P. Gunnasegaran, Influence of the oblique fin arrangement on the fluid flow and thermal performance of liquid cold plate, Case Stud. Thermal Eng. 12 (2018) 717–727.

[25]. S. Wiriyasart, P. Naphon, Liquid impingement cooling of cold plate heat sink with different fin configurations: High heat flux applications, Int. J. Heat Mass Tran. 140 (2019) 281–292.

[26]. Q. Zhang, Z. Feng, J. Zhang, F. Guo, S. Huang, Z. Li, Design of a mini-channel heat sink for high-heat-flux electronic devices, Appl. Therm. Eng. 216 (2022), 119053.

[27]. A.A. Imran, N.S. Mahmoud, H.M. Jaffal, Analysis of channel configuration effects on heat transfer enhancement in streamline-shaped cold plates used in battery cooling system: a comparative study , Int. Commun. Heat Mass Transf. 155 (2024) 107570.

[28]. J. Ren, X. Qiu, S. Wang, A liquid cooling plate based on topology optimization and bionics simplified design for battery cooling, J Energy Storage 102 (2024) 114171.

[29]. W. Jiang, J. Zhao, Z. Rao, Heat transfer performance enhancement of liquid cold plate based on mini V-shaped rib for battery thermal management, Appl. Therm. Eng. (2021), 116729.

[30]. J. Pandey, A. Husain, M. Zahid Ansari, N. Al-Azri, Performance analysis of cold plate heat sink with parallel channel and pin-fin, Mater. Today: Proc. 44 (2021) 3144–3149.

[31]. T.H. Shih, J. Zhu, J.L. Lumley, A new Reynolds stress algebraic equation model, Comput. Methods Appl. Mech. Eng. 125 (1995) 287–302.